Formation of As-As bond and its effect on absence of superconductivity in the collapsed tetragonal phase of $Ca_{0.86}Pr_{0.14}Fe_2As_2$: An optical spectroscopy study

Run Yang,[1] Congcong Le,[1] Lei Zhang,[2] Bing Xu,[1] Wei Zhang,[1,3] Kashif Nadeem,[1,4] Hong Xiao,[1] Jiangping Hu,[1,5] and Xianggang Qiu[1,5,*]

[1]*Beijing National Laboratory for Condensed Matter Physics, National Laboratory for Superconductivity, Institute of Physics, Chinese Academy of Sciences, P.O. Box 603, Beijing 100190, China*

[2]*High Magnetic Field Laboratory, Chinese Academy of Sciences, Hefei 230031, China*

[3]*College of Physics, Optoelectronics and Energy & Collaborative Innovation Center of Suzhou Nano Science and Technology, Soochow University, Suzhou 215006, China*

[4]*Department of Physics, International Islamic University, H-10, Islamabad, Pakistan*

[5]*Collaborative Innovation Center of Quantum Matter, Beijing 100084, China*

(Received 9 February 2015; published 10 June 2015)

The temperature dependence of in-plane optical conductivity has been investigated for $Ca_{0.86}Pr_{0.14}Fe_2As_2$, which shows a structural transition from tetragonal (T) to collapsed tetragonal (cT) phase at $T_{cT} \sim 73$ K. Upon entering the cT phase, drastic change characterized by the formation of a midinfrared peak near 3200 cm^{-1} (0.4 eV) in the optical conductivity is observed. Analysis of the spectral weight reveals reduced electron correlation after the cT phase transition. Based on the calculated band structure and simulated optical conductivity, we attribute the new feature around 0.4 eV to the formation of an interlayer As-As bond. The As-As bond strongly affects the Fe-As hybridizations and, in turn, drastically changes the $Ca_{0.86}Pr_{0.14}Fe_2As_2$ into a nonmagnetic Fermi liquid system without bulk superconductivity in the cT phase.

DOI: 10.1103/PhysRevB.91.224507 PACS number(s): 72.15.−v, 74.70.−b, 78.30.−j

Electron correlation and magnetism are widely believed to be intimately related to the pairing mechanism of unconventional high-temperature superconductors [1]. The iron pnictides are newly discovered superconductors with T_c as high as 55 K [2]. Similar to the cuprates, superconductivity in iron pnictides appears in the vicinity of an antiferromagnetic (AFM) phase by doping or pressure. However, the parent compounds of iron pnictides are bad metals with moderate correlation, and the local magnetic moment in iron pnictides is much larger than that in the cuprates. The strong magnetism and moderate correlation provide us an alternative material to investigate the interplay among electron correlation, magnetism, and superconductivity [3].

Up to now, there is growing evidence that the covalent Fe-As bond plays an important role in the appearance of superconductivity in iron pnictides [4]. It not only transports the carriers to tune the correlation [5], but also delivers the antiferromagnetic superexchange interactions to form the collinear antiferromagnetic order and induces spin fluctuation [6]. In addition, first-principles calculations point out that the Fe local moment is strongly sensitive to the Fe-As distance, which is influenced by the covalent Fe-As bonding [7]. Therefore, the Fe-As bonding is one of the key elements for understanding the correlation, magnetism, as well as superconductivity in iron pnictides.

Among the Fe-As based superconductors, $CaFe_2As_2$ is an excellent prototype material to explore the nature of the superconducting mechanism due to its strong Fe-As bonding and large structural instability [8–10]. At ambient pressure, it crystallizes in the tetragonal structure at room temperature and manifests a strongly first-order, concomitant structural-magnetic phase transition to an orthorhombic phase with stripelike antiferromagnetic order at 170 K [11]. Charge doping and hydrostatic pressure can suppress the AFM order and induce superconductivity in it [12]. However, when the pressure exceeds 0.35 GPa, $CaFe_2As_2$ undergoes a remarkable structural transition from the orthorhombic phase directly into the so-called collapsed tetragonal phase [13], which can also be stabilized at ambient pressure by introducing chemical pressure [14] or postannealing treatment [8]. This transition is characterized by the formation of an interlayer As-As bond and a shrinkage of the c axis by approximately 10% without breaking any symmetries [14]. In contrast to the tetragonal phase at high temperatures, neutron scattering and nuclear magnetic resonance demonstrated that the local Fe moment [15] and the spin fluctuation are quenched in the collapsed-tetragonal (cT) phase [16]. Recent transport measurements further revealed that following the lattice-collapse transition, Fermi-liquid behavior abruptly recovers along with the disappearance of bulk superconductivity [13,17]. Very recently, first-principles calculations also show that the hybridizations between Fe 3d orbitals and As 4p orbitals were also greatly affected by the newly formed As-As bond across the phase transition [5,18]. These results suggest that the vanishing of the correlation effect and magnetism may be strongly connected to the formation of the As-As bond between adjoint layers.

In this work we carried out transport, optical-spectral measurements in a Pr-doped $CaFe_2As_2$ system. The single-crystal $Ca_{0.86}Pr_{0.14}Fe_2As_2$ undergoes a first-order transition to the cT phase at 73 K. A drastic spectral change across the phase transition due to a band reconstruction is observed by the optical spectroscopy measurement [19]. The spectral weight analysis reveals a reduced correlation and a newly formed midinfrared peak at 0.4 eV in the cT phase. Compared with the theoretical results from first-principles calculations, we find that this midinfrared peak is associated with the formation of an interlayer As-As bond, which strongly affects the Fe-As

*xgqiu@iphy.ac.cn

hybridizations and changes the material to a nonmagnetic Fermi-liquid system without bulk superconductivity.

High-quality single crystals of $Ca_{1-x}Pr_xFe_2As_2$ with nominal concentration of $x = 0.14$ were synthesized by the FeAs self-flux method and the typical size was about $10\times10\times0.1$ mm^3 [20]. The composition x determined by inductively coupled plasma emission spectrometry (ICP) was about 0.135 ± 0.05. The lattice structure was detected by x-ray diffraction (XRD) (Bruker D8 Advance Instruments) using Cu $K\alpha$ ($\lambda = 0.154$ nm) radiation at various temperatures upon warming. Resistivity measurement was carried out on a Quantum Design physical property measurement system (PPMS). Magnetization was measured using a Quantum Design superconducting quantum interference device (SQUID). The reflectivity from the cleaved surface was measured at a near-normal angle of incidence on a Fourier transform infrared spectrometer (Bruker 80v) for light polarized in the *ab* planes using an *in situ* evaporation technique [21]. Data from 40 to 15 000 cm^{-1} were collected at eight different temperatures from 15 to 300 K on an ARS-Helitran cryostat. The reflectivity in the visible and UV range (10 000–40 000 cm^{-1}) at room temperature was taken with an Avaspec 2048×14 optical fiber spectrometer. The optical conductivity was determined from a Kramers-Kronig analysis of reflectivity $R(\omega)$ over the entire frequency range. A Hagen-Rubens relation ($R = 1 - A\sqrt{\omega}$) was used for low-frequency extrapolation. Above the highest measured frequency (40 000 cm^{-1}), $R(\omega)$ is assumed to be constant up to 40 eV, above which a free-electron response (ω^{-4}) is used [22].

In Fig. 1(a) we calculated the *c*-axis parameter of $Ca_{0.86}Pr_{0.14}Fe_2As_2$ from the XRD data, a great shrinkage below 75 K indicates the lattice collapse transition [14]. Correspondingly, a sudden drop is observed near 73 K in its in-plane resistivity [shown in the main panel of Fig. 1(b)]. The thermal hysteretic loop in the inset of Fig. 1(b) indicates the first-order nature of this transition. From the dc magnetic susceptibility [shown in Fig. 1(c)], a kink combined with a thermal hysteresis can also be found near 73 K. Even though obvious drops at 46 K and zero-resistance behavior at 21 K are observed in the resistance curve [23], the shielding volume fraction estimated from the field-cooling curve and zero-field-cooling curve in the inset of Fig. 1(c) is about 10%, which is much smaller than that expected for a bulk superconductor [14]. Furthermore, the superconductivity is easily suppressed by a magnetic field of 1 T, suggesting its interfacial or filamentary nature [24].

The measured in-plane reflectivity $R(\omega)$ and the real part of the in-plane optical conductivity $\sigma_1(\omega)$ are presented in Fig. 2, respectively, for selected temperatures above and below T_{cT}. The reflectivity shows a typical metallic response, approaching unity at low frequencies (<1000 cm^{-1}) and increasing upon cooling. Upon entering the cT phase, $R(\omega)$ in the midinfrared range (1000–3000 cm^{-1}) is greatly suppressed. As a consequence, the reflectivity edges at about 1000 cm^{-1} become sharper, suggesting a suppression of the carrier scattering. As suggested by Basov and Timusk [25] and Pratt *et al.* [26], the scattering could be caused by spin fluctuation; shaper reflectivity edges also indicate diminishing spin fluctuation in the cT phase. The drastic change could also be seen from the optical conductivity data in Fig. 2(b);

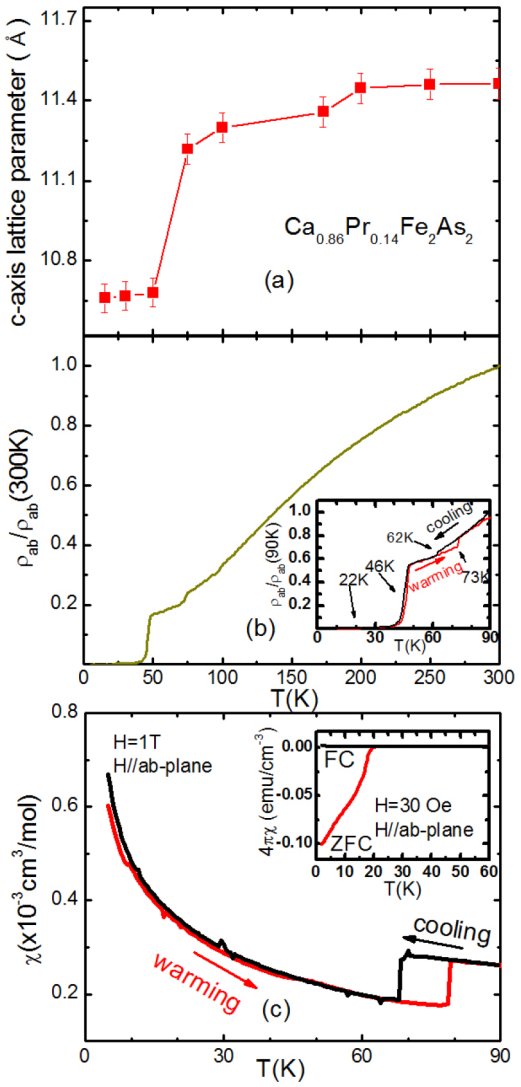

FIG. 1. (Color online) (a) Temperature dependence of lattice parameter c at various temperatures upon warming. (b) Temperature dependence of normalized resistivity of $Ca_{0.86}Pr_{0.14}Fe_2As_2$. The inset plots enlarged low-temperature data. (c) Temperature dependence of magnetic susceptibility $Ca_{0.86}Pr_{0.14}Fe_2As_2$with $H \parallel ab$ plane at 1 T. The inset shows the zero-field-cooled and field-cooled data of $Ca_{0.86}Pr_{0.14}Fe_2As_2$ at 30 Oe.

below T_{cT}, an abrupt decrease in the conductivity between 1000 cm^{-1} and 2500 cm^{-1} and a peak at 3500 cm^{-1} (~0.4 eV) are observed. (See Appendix A for more detail.) Similar behaviors have also been observed in the $R(\omega,T)$ and $\sigma_1(\omega,T)$ data of P-doped $CaFe_2As_2$ which have been attributed to an abrupt band reconstruction across the cT transition [19].

To quantitatively analyze the optical data of $Ca_{0.86}Pr_{0.14}Fe_2As_2$, we fit $\sigma_1(\omega,T)$ with a simple Drude-Lorentz mode [22,27],

$$\epsilon(\omega) = \epsilon_\infty - \sum_i \frac{\Omega_{p,i}^2}{\omega^2 + \frac{i\omega}{\tau_i}} + \sum_j \frac{\Omega_j^2}{\omega_j^2 - \omega^2 - \frac{i\omega}{\tau_i}}, \quad (1)$$

where ϵ_∞ is the real part of the dielectric function at high frequencies, the second term corresponds to the Drude response characterized by a plasma frequency $\Omega_{p,i}^2 = 4\pi ne^2/m^*$, with

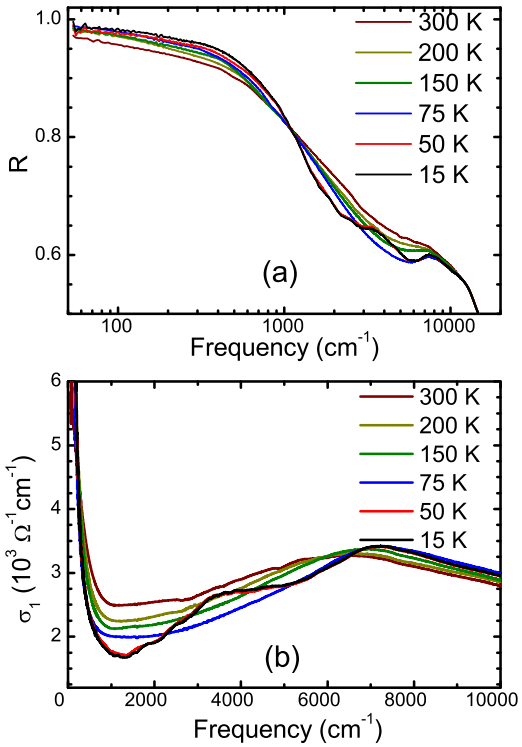

FIG. 2. (Color online) Reflectivity (a) and optical conductivity (b) of $Ca_{0.86}Pr_{0.14}Fe_2As_2$ at various temperatures.

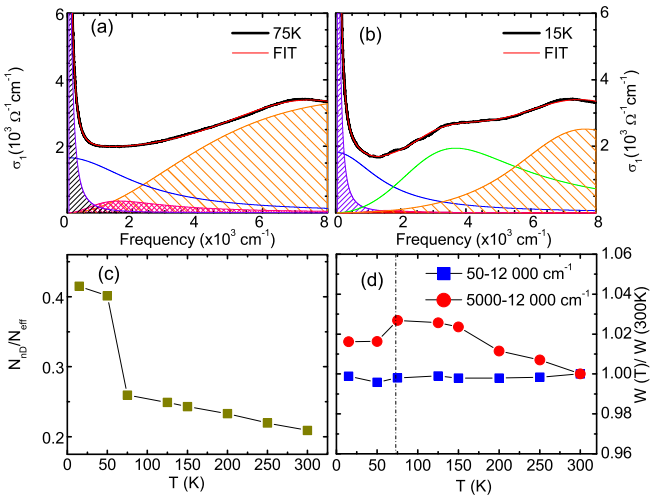

FIG. 3. (Color online) (a), (b) Optical conductivity of $Ca_{0.86}Pr_{0.14}Fe_2As_2$ at 75 K (T phase) and 15 K (cT phase) (thick black lines), fitting with the Drude-Lorentz model (thin red lines) and its decomposition into individual Drude and Lorentz terms. (c) Weights of the narrow Drude component (N_{nD}) and the total weights of the narrow and broad Drude components (N_{eff}) for various temperatures. (d) Temperature dependence of the spectral weight $W_{\omega_a}^{\omega_b} = \int_{\omega_a}^{\omega_b} \sigma_1(\omega) d\omega$ between different lower and upper cutoff frequencies. The vertical dashed line denotes T_{cT}.

n a carrier concentration and m^* an effective mass, and $1/\tau_i$ is the scattering rate. The third term is a sum of Lorentz oscillators characterized by a resonance frequency ω_j, a linewidth γ_j, and an oscillator strength Ω_j. The Drude term accounts for the free carrier (intraband) response, while the Lorentz contributions represent the interband excitations [28,29]. The fitting results shown in Figs. 3(a) and 3(b) can well reproduce the experimental results, regardless of the detailed band structure.

From the fitting results of Figs. 3(a) and 3(b) (see more results in the Appendix B), we find that the optical conductivity at low frequency (<2000 cm^{-1}) is dominated by two Drude (intraband) responses, a broad one and a narrow one, reflecting the multiorbital nature of the iron pnictides. (See Appendix B for detailed fitting results.) The narrow Drude item represents the response of the coherent carriers, corresponding to the electron pockets. The other Drude component with an extremely broad width of 2300 cm^{-1} or more is originated from a highly incoherent scattering and is dominated by the hole pockets at the center of the Brillouin zone [22,27]. It has been pointed out that the fraction of coherent Drude weight $N_{nD} = \frac{2m_0V}{\pi e^2} \int_0^\infty \sigma_{nD}(\omega) d\omega$, in which m_0, V, and σ_{nD} denote the free-electron mass, the cell volume, and the narrow Drude component, respectively, at low frequency represents the degree of coherence. Here we define N_{eff} as the sum of the weight of the narrow and broad Drude components in order to estimate the low-energy intraband response [30]. Since the electronic correlation has been regarded as a source of incoherence in iron arsenides, N_{nD}/N_{eff} could also be a measure of the strength of electronic correlations [30]. The data of N_{nD}/N_{eff} in Fig. 3(c) shows an abrupt enhancement of the degree of coherence across the T to cT phase transition, suggesting a weakening of electronic correlation.

Then we focus on the optical conductivity $\sigma_1(\omega)$ at high frequencies (above 5000 cm^{-1}). It has been reported that in iron pnictides the spectral weight at low frequency would transfer to a high-energy area (>0.5 eV) as temperature goes down. This behavior is widely attributed to the Hund's rule coupling effect [31,32], which can localize and polarize the itinerant electrons to enhance the correlation and local moment. To investigate the anomalous spectral weight transfer, we have calculated and normalized the spectral weight between different lower and upper cutoff frequencies. From the results shown in Fig. 3(d), it can be found that the overall spectral weight between 50 and 12 000 cm^{-1} is temperature independent [33], while the spectral weight at high frequency (5000∼12 000 cm^{-1}) varies significantly with the temperature, suggesting that there indeed exists an obvious Hund's rule coupling effect. Above T_{CT}, more low-frequency spectral weight transfers to the high-energy area (>5000 cm^{-1}) with decreasing temperature, but after the phase transition, this tendency is suppressed. The spectral weight above 5 000 cm^{-1} starts to decline, indicating the weakening of the Hund's coupling effect, which can lead to weaker correlation and a smaller Fe local moment [34].

A remarkable feature we observed in the optical spectra is the newly formed midinfrared peak around 0.4 eV after the phase transition. By comparing the optical-spectral data of $CaCu_2As_2$, which has an intrinsic As-As interlayer bond [35], we suppose that this new feature may be associated with the formation of an As-As bond in the cT phase. To confirm this hypothesis, we have calculated the band structure and simulated the optical conductivity in different situations. The

calculations are performed using density functional theory (DFT) as implemented in the Vienna *ab initio* simulation package (VASP) code [36–38]. The generalized-gradient approximation (GGA) for the exchange correlation functional is used [39]. Throughout the work, the cutoff energy is set to be 400 eV for expanding the wave functions into a plane-wave basis £¬and the numbers of these k points are 16 16 8. Furthermore, the experimental parameters [5] ($a_T = 3.891\,5$ Å, $c_T = 11.690$ Å, $a_{cT} = 3.979\,2$ Å, $c_{cT} = 10.607\,3$ Å;) were used in the calculation. The results are shown in Fig. 4; the simulated optical conductivities agree well with the observed conductivities in both the T and cT phase qualitatively (more detail results could be seen in Appendix C). Then we enlarge the interlayer distance without changing the intralayer structure in the cT phase. When the distance exceeds 3.0 Å, the antibonding state sinks below the Fermi level [Fig. 4(c)], corresponding to the destroyed As-As bond. Simultaneously, the midinfrared peak [as illustrated in Fig. 4(e) by the green arrow] in the simulated optical conductivity disappears [Fig. 4(f)]. This provides strong evidence that the midinfrared peak around 0.4 eV is associated with the interlayer As-As bond. From the optical conductivities [Fig. 2(b)] and their fitting results [Figs. 3(a) and 3(b)], we find that the newly formed 0.4-eV peak seems to absorb the spectral weight of the broad Drude item at low frequency and frustrate the spectral weight transfer from a low- to high-frequency area. Hence, we infer that the As-As bond may relate to the weaker correlation, quenched magnetism as well as the disappeared bulk superconductivity in the cT phase.

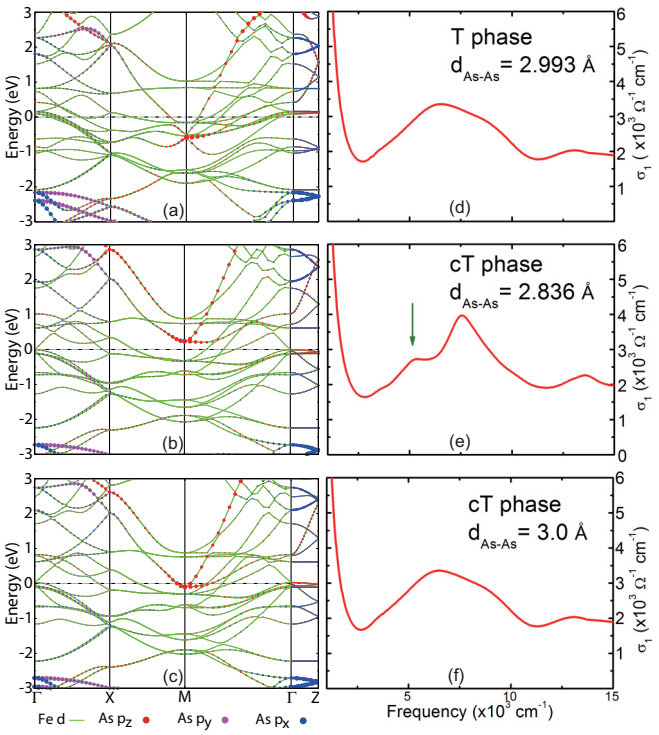

FIG. 4. (Color online) The calculated band structure and simulated optical conductivity in the T phase (a), (d) and cT phase (b), (e). (c), (f) Results calculated with enlarged interlayer distance and unchanged intralayer structure of that in the cT phase. See the text for more detail.

According to the calculated band structure [Figs. 4(a)–4(c)], the bonding-antibonding splitting of As p_x/p_y orbitals around the Γ point is found to be enlarged after the cT phase transition, suggesting increased overlap between Fe d_{xy} orbitals and As p_x/p_y orbitals [4] due to the shorter Fe-As covalent bond induced by the formation of the As-As bond [14]. The enhanced overlap will make the electrons, especially those in the d_{xy} orbitals, more itinerant and greatly weakens the correlation [5,40]. Since the Fe spin polarization is driven by the on-site (Hund) exchange [4], the more itinerant electrons hardly form the local moment. Thus the shorter Fe-As bond (<2.36 Å [14]) is responsible for the weaker correlation and quenched local moment [7]. On the other hand, around the M point, the As p_z orbitals, which are located under the Fermi level and hybridize well with the Fe 3d orbitals in the T phase [Fig. 4(a)], have been pushed above the Fermi level and are decoupled with the Fe 3d orbitals after the cT phase transition [Fig. 4(b)]. Previous research pointed out that the As-As bond perpendicular to the Fe layer was dominated by the As p_z orbitals [41], and thus the empty antibonding states of As p_z orbitals in Fig. 4(b) correspond to the formation of As-As bond in the cT phase. Since the hybridizations between the As p_z orbitals and the Fe 3d orbitals deliver the antiferromagnetic superexchange interaction between the nearest and next-nearest Fe atoms to form the AFM order and to induce the spin fluctuation [6], the decoupling effect caused by the newly formed interlayer As-As bond greatly frustrates the antiferromagnetic interaction and, in turn, eliminates the AFM order and spin fluctuation in the cT phase. In addition, the bulk superconductivity disappearing with the spin fluctuation supports the notion of a coupling between spin fluctuations and unconventional superconductivity in the iron pnictides [3,16]. Accordingly, the newly formed As-As hybridization plays a decisive role in suppressing the correlation, magnetism, and superconductivity in the cT phase by affecting the Fe-As hybridization.

In summary, we report detailed transport and optical study results on a $Ca_{0.86}Pr_{0.14}Fe_2As_2$ single crystal which undergoes structural phase transition from a tetragonal to a collapsed tetragonal phase. After the cT phase transition, the sharper reflectance edge and great spectral weight redistribution in the optical conductivity reflect suppressed spin fluctuation and weaker electron correlation. Based on the fist-principles calculation, we confirm that the newly formed feature around 0.4 eV is caused by the interlayer As-As bonding. The formation of an As-As bond in the cT phase weakens the correlation, quenches the local moment, and frustrates the dynamical spin fluctuation by affecting the Fe-As hybridization. Since the superconductivity in iron pnictides is widely believed to be mediated by the spin fluctuation, the degree of hybridization between iron and arsenic atoms can provide a possible explanation for the lack of bulk superconductivity in the cT phase.

The authors thank Pengcheng Dai, Yaomin Dai, Bohong Li, and Fei Cheng for useful discussion, and we thank Yuping Sun, Minghu Fang, and Hangdong Wang for assistance with x-ray diffraction measurements. This work was supported by the NSFC (Grant No. 91121004 and 973 Project No. 2015CB921303) and the MOST (973 Projects No. 2012CB21403, No. 2011CBA00107, No. 2012CB921302, and No. 2015CB929103).

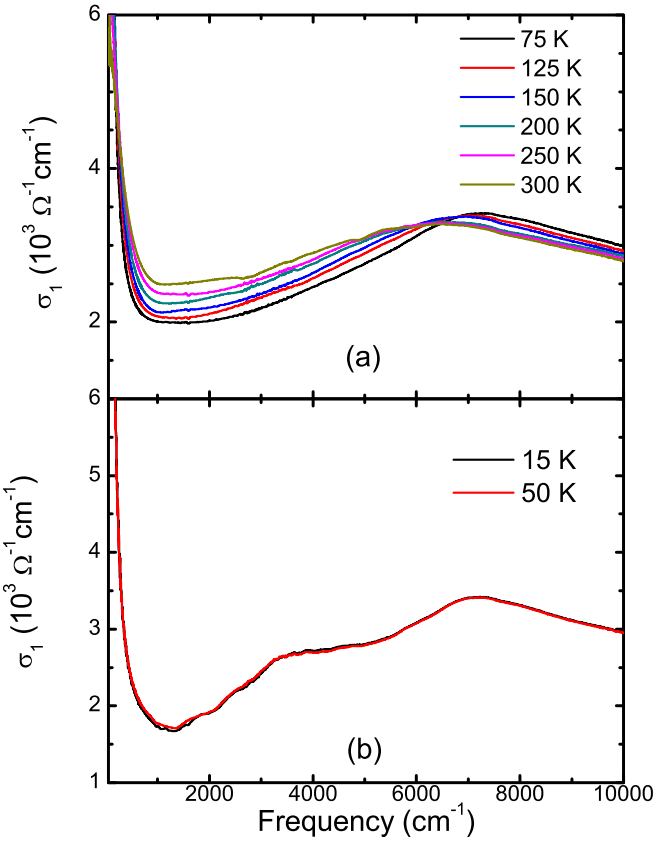

FIG. 5. (Color online) Optical conductivity with all measured temperatures above 75 K (a) and one below 75 K (b).

APPENDIX A: OPTICAL CONDUCTIVITY BEFORE AND AFTER THE LATTICE COLLAPSE TRANSITION

In Fig. 5 we present all the measured optical conductivities in two pictures, one with all measured temperatures above 75 K and one below 75 K. The optical conductivity of $Ca_{0.86}Pr_{0.14}Fe_2As_2$ in the normal state (>75 K) shows typical features of 122 iron pnictides. The peaklike structure around 6000 cm^{-1} has been regarded as a high-energy pseudogap which relates to the Hund's rule coupling effect. From 300 to 75 K this peak shifts from 6000 to 7000 cm^{-1}. This peak shifting is common in Ba122 and Sr122 systems [31], but the range is wider in our sample. The reason for such a large shifting range is still unknown. We think that this anomalous shifting may be related to the structural instability and the spin state transition in rare-earth-doped $CaFe_2As_2$ [10] and requires further investigation.

APPENDIX B: THE DETAIL FITTING RESULTS

To quantitatively analyze the optical data, we fitted the optical conductivity with a generally used two-Drude model; the results are shown in Fig. 6. The subscript n and b stand for the narrow and broad Drude terms, respectively. From the results, we find that, upon entering the cT phase, the plasma frequency and the scattering rate of the broad Drude term shows an abrupt decrease, suggesting remarkable shrinkage of the broad Drude as well as the hole pockets which are caused by formation of the As-As bond.

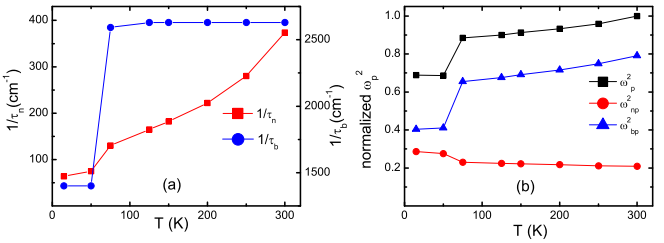

FIG. 6. (Color online) Temperature dependence of ω_p^2 (a) normalized to the value of 300 K and scattering rate $1/\tau$, and (b) of the two Drude terms of $Ca_{0.86}Pr_{0.14}Fe_2As_2$.

APPENDIX C: MORE CALCULATED RESULTS

To demonstrated whether the interlayer distance could greatly affect the position of the newly formed midinfrared peak in the cT phase, we calculated the optical conductivity with the interlayer distance of 2.90 Å. The results are shown in

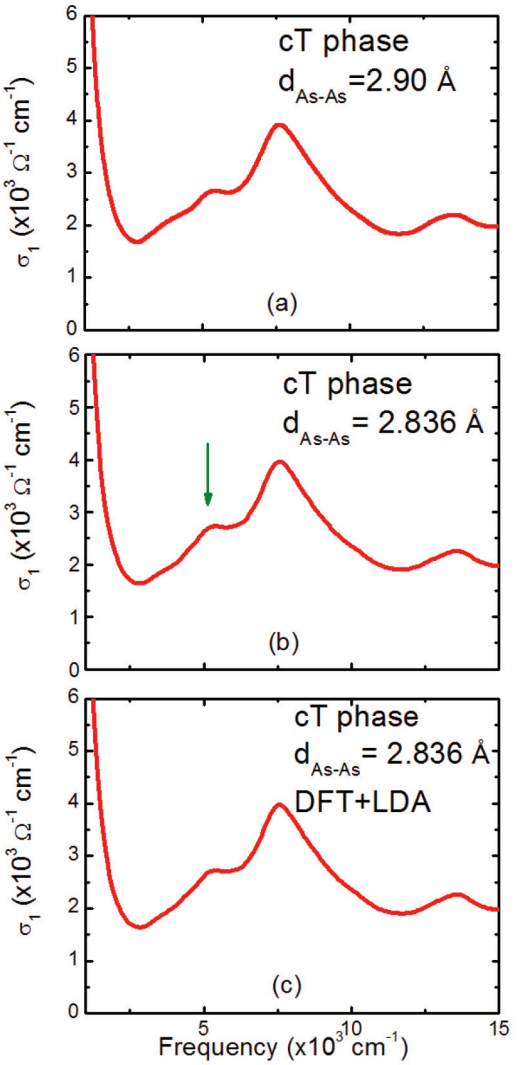

FIG. 7. (Color online) (a), (b) Simulated optical conductivity with different interlayer distance. (c) Optical conductivity calculated with the local density approximation for the exchange potential.

Fig. 7. By comparing the results of 2.83 Å, we do not observe obvious shifting of the newly formed midinfrared structure. We infer that the difference may not be caused by the different interlayer distance. Very recently, Mandal *et al.* has calculated the optical conductivity in the cT phase based on DFT+DMFT (dynamical mean field theory) [34]. The calculated data precisely reproduced the experimental data. The discrepancy of our data may come from the strong correlation, which is underestimated in our calculation. However, the correlation does not affect the formation of the As-As bond in the cT phase, and our calculation can qualitatively reflect the nature of the sample in the cT phase.

[1] P. A. Lee, N. Nagaosa, and X.-G. Wen, Rev. Mod. Phys. **78**, 17 (2006).
[2] D. C. Johnston, Adv. Phys. **59**, 803 (2010).
[3] J. Paglione and R. L. Greene, Nat. Phys. **6**, 645 (2010).
[4] K. D. Belashchenko and V. P. Antropov, Phys. Rev. B **78**, 212505 (2008).
[5] J. Diehl, S. Backes, D. Guterding, H. O. Jeschke, and R. Valentí, Phys. Rev. B **90**, 085110 (2014).
[6] F. Ma, Z.-Y. Lu, and T. Xiang, Phys. Rev. B **78**, 224517 (2008).
[7] S. Mirbt, B. Sanyal, C. Isheden, and B. Johansson, Phys. Rev. B **67**, 155421 (2003).
[8] B. Saparov, C. Cantoni, M. Pan, T. C. Hogan, W. Ratcliff, S. D. Wilson, K. Fritsch, B. D. Gaulin, and A. S. Sefat, Sci. Rep. **4**, 4120 (2014).
[9] D. A. Tompsett and G. G. Lonzarich, arXiv:0902.4859.
[10] H. Gretarsson, S. R. Saha, T. Drye, J. Paglione, J. Kim, D. Casa, T. Gog, W. Wu, S. R. Julian, and Y.-J. Kim, Phys. Rev. Lett. **110**, 047003 (2013).
[11] P. Canfield, S. Budko, N. Ni, A. Kreyssig, A. Goldman, R. McQueeney, M. Torikachvili, D. Argyriou, G. Luke, and W. Yu, Phys. C (Amsterdam, Neth.) **469**, 404 (2009).
[12] M. S. Torikachvili, S. L. Bud'ko, N. Ni, and P. C. Canfield, Phys. Rev. Lett. **101**, 057006 (2008).
[13] W. Yu, A. A. Aczel, T. J. Williams, S. L. Bud'ko, N. Ni, P. C. Canfield, and G. M. Luke, Phys. Rev. B **79**, 020511 (2009).
[14] S. R. Saha, N. P. Butch, T. Drye, J. Magill, S. Ziemak, K. Kirshenbaum, P. Y. Zavalij, J. W. Lynn, and J. Paglione, Phys. Rev. B **85**, 024525 (2012).
[15] L. Ma, G. F. Ji, J. Dai, S. R. Saha, T. Drye, J. Paglione, and W.-Q. Yu, Chin. Phys. B **22**, 057401 (2013).
[16] J. H. Soh, G. S. Tucker, D. K. Pratt, D. L. Abernathy, M. B. Stone, S. Ran, S. L. Bud'ko, P. C. Canfield, A. Kreyssig, R. J. McQueeney, and A. I. Goldman, Phys. Rev. Lett. **111**, 227002 (2013).
[17] S. Kasahara, T. Shibauchi, K. Hashimoto, Y. Nakai, H. Ikeda, T. Terashima, and Y. Matsuda, Phys. Rev. B **83**, 060505 (2011).
[18] T. Yildirim, Phys. Rev. Lett. **102**, 037003 (2009).
[19] X. B. Wang, H. P. Wang, T. Dong, R. Y. Chen, and N. L. Wang, Phys. Rev. B **90**, 144513 (2014).
[20] F. Ronning, T. Klimczuk, E. D. Bauer, H. Volz, and J. D. Thompson, J. Phys.: Condens. Matter **20**, 322201 (2008).
[21] C. C. Homes, M. Reedyk, D. A. Cradles, and T. Timusk, Appl. Opt. **32**, 2976 (1993).
[22] Y. M. Dai, A. Akrap, J. Schneeloch, R. D. Zhong, T. S. Liu, G. D. Gu, Q. Li, and C. C. Homes, Phys. Rev. B **90**, 121114 (2014).
[23] B. Lv, L. Deng, M. Gooch, F. Wei, Y. Sun, J. K. Meen, Y.-Y. Xue, B. Lorenz, and C.-W. Chu, Proc. Natl. Acad. Sci. USA **108**, 15705 (2011).
[24] K. Gofryk, M. Pan, C. Cantoni, B. Saparov, J. E. Mitchell, and A. S. Sefat, Phys. Rev. Lett. **112**, 047005 (2014).
[25] D. Basov and T. Timusk, Rev. Mod. Phys. **77**, 721 (2005).
[26] D. K. Pratt, Y. Zhao, S. A. J. Kimber, A. Hiess, D. N. Argyriou, C. Broholm, A. Kreyssig, S. Nandi, S. L. Bud'ko, N. Ni, P. C. Canfield, R. J. McQueeney, and A. I. Goldman, Phys. Rev. B **79**, 060510 (2009).
[27] D. Wu, P. G. Khalifah, D. G. Mandrus, and N. L. Wang, J. Phys.: Condens. Matter **20**, 325204 (2008).
[28] P. Marsik, C. N. Wang, M. Rössle, M. Yazdi-Rizi, R. Schuster, K. W. Kim, A. Dubroka, D. Munzar, T. Wolf, X. H. Chen, and C. Bernhard, Phys. Rev. B **88**, 180508 (2013).
[29] M. J. Calderón, L. d. Medici, B. Valenzuela, and E. Bascones, Phys. Rev. B **90**, 115128 (2014).
[30] S. Nakajima, M. Ishida, T. Tanaka, and S.-i. Uchida, J. Phys. Soc. Jpn. **83**, 104703 (2014).
[31] N. L. Wang, W. Z. Hu, Z. G. Chen, R. H. Yuan, G. Li, G. F. Chen, and T. Xiang, J. Phys.: Condens. Matter **24**, 294202 (2012).
[32] A. A. Schafgans, S. J. Moon, B. C. Pursley, A. D. LaForge, M. M. Qazilbash, A. S. Sefat, D. Mandrus, K. Haule, G. Kotliar, and D. N. Basov, Phys. Rev. Lett. **108**, 147002 (2012).
[33] Since the high energy ($>12000\,\mathrm{cm}^{-1}$) optical spectra we observed does not vary with the temperature, we do not take the spectral weight in this area into consideration.
[34] S. Mandal, R. E. Cohen, and K. Haule, Phys. Rev. B **90**, 060501 (2014).
[35] B. Cheng, B. F. Hu, R. Y. Chen, G. Xu, P. Zheng, J. L. Luo, and N. L. Wang, Phys. Rev. B **86**, 134503 (2012).
[36] G. Kresse and J. Furthmüller, Comput. Mater. Sci. **6**, 15 (1996).
[37] G. Kresse and J. Hafner, Phys. Rev. B **47**, 558 (1993).
[38] G. Kresse and J. Furthmüller, Phys. Rev. B **54**, 11169 (1996).
[39] J. P. Perdew, K. Burke, and M. Ernzerhof, Phys. Rev. Lett. **77**, 3865 (1996).
[40] Z. P. Yin, K. Haule, and G. Kotliar, Nat. Mater. **10**, 932 (2011).
[41] R. Hoffmann and C. Zheng, J. Phys. Chem. **89**, 4175 (1985).